Spatial Distributions of Mean Age and Higher Moments in Steady Continuous Flows

M. Liu and J. N. Tilton
DuPont Engineering, DuPont Co., Wilmington, DE 19898

DOI 10.1002/aic.12151
Published online April 20, 2010 in Wiley Online Library (wileyonlinelibrary.com).

Transport equations and boundary conditions for spatial distribution of age moments in steady continuous flows are derived. Mean age is the first moment. The coefficient of variation is obtained from the second moment. Mixing-cup averaged mean age and higher moments across the exit plane are identical to the corresponding moments of the residence-time distribution. Numerical solutions for a 2-D (two-dimensional) reactor are studied and compared with those from a transient tracer equation. Agreement is excellent. Local tracer distribution function curves reveal that mean age is located on the long tail for both convection dominated short circuiting paths and diffusion dominated dead zones. Computing cost for the mean age and higher moment equations is orders of magnitude lower than that for the transient tracer concentration equation, making this mean age method an efficient tool to study mixing in steady continuous flow systems. © 2010 American Institute of Chemical Engineers *AIChE J,* 56: 2561–2572, 2010

Keywords: age, mean age, residence time distribution, moments, CFD, mixing

Introduction

Residence time distribution (RTD) is a useful indicator of mixing behavior in continuous flow process equipment.[1,2,3] Cumulative distribution functions $F(t)$ and differential distribution or frequency functions $f(t)$ are typically used to represent RTD, with $F(t)$ being the fraction of fluid exiting a vessel with residence time less than or equal to t and $f(t)dt$ being the fraction of fluid exiting with residence time between t and $t+dt$. For steady incompressible flows, these distribution functions may be obtained by measuring exit concentration response to prescribed tracer inputs. An ideal tracer is one which does not alter the velocity distribution, and has diffusivity equal to the self-diffusivity of the bulk fluid. The most widely used tracer input functions are Dirac delta (pulse) and step functions. For pulse input, the distributions may be obtained from the exit concentration response $C_{\text{out}}(t)$. More precisely, the exit concentration $C_{\text{out}}(t)$ is the mixing cup (flow-weighted) average concentration across the exit plane

$$F = \frac{\int_0^t C_{\text{out}} dt'}{\int_0^\infty C_{\text{out}} dt} = \int_0^t f dt' \tag{1}$$

$$f = \frac{C_{\text{out}}}{\int_0^\infty C_{\text{out}} dt} = \frac{dF}{dt} \tag{2}$$

The F curve may also be obtained directly from the exit concentration response to a step-function input of tracer. In addition to the requirements of steady incompressible flow, these relations also require the system to be closed. A closed system is one with no backflow, diffusion or dispersion of tracer through inlet and outlet surfaces. The term "E-curve" or $E(t)$ is also in common use for $f(t)$.

The mean residence time is the first moment of f

$$\bar{t} = \frac{\int_0^\infty t C_{\text{out}} dt}{\int_0^\infty C_{\text{out}} dt} = \int_0^\infty t f dt \tag{3}$$

Correspondence concerning this article should be addressed to M. Liu at minye.liu@usa.dupont.com, and J. N. Tilton at james.n.tilton@usa.dupont.com.

Danckwerts[4] is widely credited for the groundwork for RTD theory, although some work had been published earlier (Gilliland and Mason[5]). While a detailed discussion of RTD theory can be found in the research literature, as well as in chemical engineering textbooks, applications of the method to industrial equipment is not routine because of the difficulty of carrying out accurate tracer response experiments.

When the RTD deviates excessively from desired ideals such as those for plug flow or perfect backmixing, adverse effects may occur. Poor yield or selectivity in chemical reactors, degradation or gel formation in polymer processing, NO_x formation in furnaces, and inadequate interfacial mass or heat transfer are just a few examples. Knowledge of the RTD can provide useful insight into the mixing performance of equipment, but there are well known shortcomings. For example, two reactor configurations with identical RTD can produce different conversion of a reaction with nonlinear kinetics.[6,7] In one case a plug flow section is followed by a perfectly backmixed (CSTR) section. In the other, the sections are reversed. They will have the same RTD but different conversion. Thus, it is often stated that RTD cannot distinguish "early mixing" from "late mixing". It may be more strongly stated that RTD provides no information in regard to the spatial distribution of mixing. The shape of the RTD may suggest the presence of dead zones or short-circuiting, but this is largely guesswork, and the location of such regions cannot be determined from the RTD. This motivates the need to understand the spatial distribution of age within the vessel, and not just the exit age.

Over the past two decades, the use of computational fluid dynamics (CFD) to determine residence time distribution has become reasonably well established as an alternative to physical tracer experiments. Two CFD methods have been employed. One is to inject a large number of passive tracer particles into the flow, follow them by Lagrangian particle tracking, and collect their exit time statistics. Another is to simulate the chemical tracer experiment, solving the transient tracer species concentration transport equation. Both require use of time-dependent solvers. Small time step sizes in applying such time-dependent solvers are critical to the accuracy of the results, while long simulation times are needed to capture the long-time tail of the distribution. This often results in long computation time, even for a steady flow. Frequently Lagrangian particle tracking RTD computations fail to capture the effects of turbulent diffusion.

Usually, the term "residence time" is reserved for molecules exiting the vessel, giving the elapsed time since they entered. The term "age" is reserved to describe the elapsed time since entrance of molecules still in the vessel. When a molecule reaches the exit, its age equals the residence time. Danckwerts[4] introduced the concept of internal age distribution. He showed that the distribution functions for the age of the entirety of the fluid still within a vessel are simply related to the exit RTD functions and the mean residence time. This internal age distribution is not spatially resolved.

Equations 1–3 are widely familiar to practitioners in the chemical reactor engineering and mixing fields. Far less well known is the fact, originally demonstrated by Danckwerts,[8] that similar equations may be applied locally at any point in the vessel, to use local tracer concentration measurements to produce spatially resolved distribution functions. Thus, the spatial age distribution functions $\tilde{f}(\mathbf{x},\alpha)$ and $\tilde{F}(\mathbf{x},\alpha)$ at position $\mathbf{x}$ are given by

$$\tilde{F} = \frac{\int_0^{\alpha} C(\mathbf{x},t)dt}{\int_0^{\infty} C(\mathbf{x},t)dt} = \int_0^{\alpha} \tilde{f}dt \tag{4}$$

$$\tilde{f} = \frac{C(\mathbf{x},\alpha)}{\int_0^{\infty} C(\mathbf{x},\mathrm{t})dt} = \frac{d\tilde{F}}{d\alpha} \tag{5}$$

Thus, $\tilde{f}(\mathbf{x},\alpha)$ is the frequency distribution of the age of molecules at the local point of interest. The fraction of molecules at point $\mathbf{x}$ with age between α and $\alpha+d\alpha$ is $\tilde{f}(\mathbf{x},\alpha)d\alpha$.

The mean age as a function of spatial position is $a(\mathbf{x})$

$$a(\mathbf{x}) = \frac{\int_0^{\infty} tC(\mathbf{x},t)dt}{\int_0^{\infty} C(\mathbf{x},t)dt} = \int_0^{\infty} t\tilde{f}dt \tag{6}$$

For brevity, the field variable $a(\mathbf{x})$ may be referred to as the mean age distribution.

Care must be taken to appreciate different uses of the word *distribution*. The function $\tilde{f}(\mathbf{x},\alpha)$ is the probability density or frequency distribution function of the independent variable age α at $\mathbf{x}$. The spatial mean age distribution refers to the spatial variation of the mean age $a(\mathbf{x})$.

It is unfortunate that the concept of the spatial distribution of mean age has remained in relative obscurity, because its measurement or computation can provide considerable insight into diagnosis and improvement of mixing conditions beyond that inferred from RTD alone. A perfectly mixed stirred tank will have a uniform spatial age distribution. Long feed plumes of low age reveal slow dispersion of a reactor feed. Dead zones can be identified as regions with age far greater than their surroundings, often far greater than the mean residence time. A dead zone is not necessarily a region of low velocity; closed circulation zones with low rates of molecular or turbulent diffusion across their boundaries will contain fluid of large age. Without the solution of spatial age distribution, even with detailed 3-D flow solutions from CFD, identifying such dead zones is not trivial. Conventional ways of examining CFD velocity fields, such as planar velocity vector plots and contour plots may lead to misinterpretation of closed circulation loops as dead zones, when in fact there may be strong exchange of fluid in the direction normal to the plane.

Just as physical and numerical tracer experiments can be used to determine the residence time distribution, they may also be employed to determine the local distribution functions $\tilde{f}(\mathbf{x},\alpha)$ and $\tilde{F}(\mathbf{x},\alpha)$, as well as the spatial mean age distribution $a(\mathbf{x})$. These methods can be experimentally and computationally challenging.

There have been a few reports on the use of a much simpler method to determine the spatial distribution of the mean age. These employ a steady transport equation for $a(\mathbf{x})$. Sandberg[9] may have been the first to derive the transport equation, following closely Spalding's[10] analysis. In fact, Spalding was just one step short of writing the equation out explicitly. This steady transport equation can be solved by CFD after the steady flow solution is obtained. The solution for mean age $a(\mathbf{x})$ by the steady-transport equation is much less computing intensive than that of transient tracer species or

tracking large numbers of passive tracer particles. Baleo and le Cloirec[11] provided an example computation of $a(\mathbf{x})$ in a turbulent flow through a channel containing a series of sudden expansions and contractions, and found excellent agreement between their computations and experimental measurements.

In the next section, a derivation of the transport equation for mean age following the approach of Spalding and Sandberg is shown. Furthermore, the theory is advanced by deriving transport equations for higher moments of the age distribution. Thus, not only can the spatial variation of the mean of the age be determined, but also the spatial variation of its variance σ^2 $(\mathbf{x})$ and higher moments. Indeed, by taking sufficient moments, the entire frequency distribution $\tilde{f}(\mathbf{x}, \alpha)$ could in principle be reconstructed. The relationship between the moments of age and residence time distributions is also discussed. Next, the numerical solution to a test problem is investigated, comparing solutions from mean age and moment equations with those from the transient tracer equation, discussing insights about the spatial distribution of mean age and higher moments, and showing numerical results confirming the key assumptions made in derivations. Finally, conclusions are presented in the last section.

Governing Equations for Mean Age and Higher Moments

Mean age

The approach of Sandberg[9] and Spalding[10] is to follow. Consider a pulse tracer injection, for a steady incompressible flow through a closed system with one inlet and one outlet, for which Eqs. 4–6 apply. The transport equation for the tracer species is

$$\frac{\partial C}{\partial t} + \nabla \cdot (\mathbf{v}C) = \nabla \cdot (D \nabla C) \tag{7}$$

Here D is the molecular diffusivity. While Eq. 7 applies to both steady and unsteady velocity fields, the analysis in this article will be restricted to steady flows. In the case of steady turbulent flows, Eq. 7 becomes the Reynolds averaged equation, where $\mathbf{v}$ and C are the Reynolds averaged velocity and concentration, and D is replaced by the effective turbulent diffusivity, $D_e = D_t + D$. Typically, the turbulent diffusivity is represented as the ratio of the turbulent momentum diffusivity, or turbulent kinematic viscosity, used to solve the Reynolds averaged momentum equation, to a Schmidt number of order unity.

There must be wide separation between the turbulence- and residence time scales to apply the tracer method to turbulent flow. In the following equations, the laminar form with only the molecular diffusion is used, but the results directly transfer to steady Reynolds averaged turbulent flow by using the turbulent effective diffusivity.

Multiplication of Eq. 7 by t and integration over time give

$$\int_0^\infty t \frac{\partial C}{\partial t} dt + \int_0^\infty \nabla \cdot (t\mathbf{v}C) dt = \int_0^\infty \nabla \cdot D \nabla (tC) dt \tag{8}$$

where t, being independent of position, has been brought inside the spatial derivatives. The first term on the lefthand side may be integrated by parts.

$$\int_0^\infty t \frac{\partial C}{\partial t} dt = tC|_0^\infty - \int_0^\infty C dt \tag{9}$$

Spalding considered steady incompressible flow in a closed system with one inlet and one outlet. He inferred that the quantity

$$I \equiv \int_0^\infty C dt \tag{10}$$

is spatially invariant.

The first term on the righthand side of Eq. 9 will be zero if tC is zero in the limit $t \to \infty$. That is, C must go to zero faster than t goes to infinity. The mean age $a = \int_0^\infty tC dt / \int_0^\infty C dt = \int_0^\infty tC dt / I$ can exist only if $tC \to 0$ as $t \to \infty$. That is, the numerator integral converges to a finite limit only if $tC \to 0$ as $t \to \infty$. It has been observed that C approaches zero exponentially in flows with both convection and diffusion, so that not only tC, but also higher powers $t^n C$ with $n > 1$ also go to zero. This will ensure the existence of higher moments of the age distribution which are considered subsequently. This behavior is investigated numerically in the next section.

With $tC|_0^\infty = 0$, substitution of Eq. 9 into Eq. 8, and division by I yields

$$-1 + \nabla \cdot \left\{ \mathbf{v} \left[\frac{\int_0^\infty tC dt}{\int_0^\infty C dt} \right] \right\} = \nabla \cdot \left\{ D \nabla \left[\frac{\int_0^\infty tC dt}{\int_0^\infty C dt} \right] \right\} \tag{11}$$

where the time invariance of $\mathbf{v}$ and D, and the spatial invariance of I have been used. The quantity in square brackets is the local mean age a by Eq. 6. Thus, the transport or conservation equation for mean age is

$$\nabla \cdot (\mathbf{v}a) = \nabla \cdot D \nabla a + 1 \tag{12}$$

For incompressible flow, this may also be written as

$$\mathbf{v} \cdot \nabla a = \nabla \cdot D \nabla a + 1 \tag{13}$$

Equation 12 is in the same conservative form as the steady transport equations for momentum, energy and species, and so can be solved with the same CFD solver. It shows that the mean age is convected and diffused.

Boundary conditions are needed for Eq. 12. These may be derived from the boundary conditions for the tracer concentration. For fluid with tracer concentration C_{in} crossing the inlet plane, where the concentration is C, at velocity v_n, the species boundary condition for an open inlet is $C_{in} = C - (D/v_n)\partial C/\partial x_n$, where x_n is the normal coordinate in the flow direction. For a closed inlet, where convection dominates over diffusion (large Peclet number) the tracer concentration is equal to the feed concentration, as noted by Danckwerts.[4] For the pulse inlet $C_{in} = C = 0$, for $t > 0$. By Eq. 6 the mean age is then zero, as expected.

$$a = 0, \quad \text{at inlet} \tag{14}$$

On solid walls, the normal gradient of tracer concentration is zero (the tracer cannot diffuse into the wall), so that $\partial C/\partial x_n = 0$, and, therefore, by Eq. 6

$$\mathbf{n} \cdot \nabla a = \frac{\partial a}{\partial x_n} = 0, \quad \text{on solid walls} \tag{15}$$

At the outlet, the Danckwerts zero normal gradient $\partial C/\partial x_n = 0$ boundary condition is generally applied to the species conservation equation. This boundary condition renders diffusion negligible compared to convection, giving a closed boundary. By Eq. 6, the corresponding boundary condition at the exit for the mean age is

$$\mathbf{n} \cdot \nabla a = \frac{\partial a}{\partial x_n} = 0, \quad \text{at outlet} \tag{16}$$

This boundary condition is consistent with the requirement for closed boundaries upon which the tracer method is dependent. As noted by Froment and Bischoff[12] the influence of the exit boundary condition on equations of this type is weak unless there is very strong diffusion (low Peclet number, or low ratio of convection to diffusion) at the exit.

The equivalence of Eq. 12 and its boundary conditions to those for the steady transport and reaction of a chemical species absent from the feed, but produced by a constant rate (zero-order) reaction may be recognized. Therefore, use of a suitably defined chemical reaction is another way to obtain the spatial distribution of mean age from a CFD code.

Volume integration of Eq. 12, after application of the divergence theorem, yields the expected result that the mixing cup (mass-flow weighted) mean age at the exit is the system volume divided by the volumetric flow rate Q for incompressible flow with closed inlets and outlets. Consider a control volume V bounded by a surface with outward unit normal $\mathbf{n}$. The surface S is comprised of solid walls S_w, inlet S_i and outlet S_e.

$$\bar{a}_e = \frac{\int_{S_e} \mathbf{n} \cdot \mathbf{v} a dS}{Q} = \frac{V}{Q} + \frac{\int_{S_w+S_i+S_e} D\mathbf{n} \cdot \nabla a dS}{Q} \tag{17}$$

With closed inlets and outlets, and zero normal gradient at the wall, the second term on the righthand side vanishes, giving $\bar{a}_e = V/Q$.

Real flows will have diffusion or dispersion across the inlet. The error in assuming a closed inlet should be negligible for convection dominated inlets as noted earlier. Based on Spalding,[10] the error in Eq. 17 remains small as long as $DS_i^2/(QV) \ll 1$. This implies a large Peclet number based on a characteristic length VS_i. Spalding arrived at the same result as Eq. 17 by analogy to the energy equation.

As noted previously, the preceding derivation could be applied to Reynolds averaged steady turbulent flow, so that Eq. 12 is replaced by its Reynolds averaged form

$$\nabla \cdot (\mathbf{v} a) = \nabla \cdot \left[\left(\frac{\nu_t}{Sc_a} + D \right) \nabla a \right] + 1 \tag{18}$$

where ν_t is the turbulent momentum diffusivity, and Sc_a is the turbulent Schmidt number for mean age. It is reasonable to set Sc_a the same as that for turbulent species diffusion, since mean age is determined by tracer diffusion. Typical turbulent Schmidt number values range from 0.7 to 1.0.

Equation for particle age

An equation similar to Eq. 13 can be derived from a starting point that does not rely on the chemical tracer method. Material (fluid) particles are defined as fictitious particles which move at the flow velocity $\mathbf{v}$, the mass-averaged velocity of the molecules at the local position of the particle. Unlike molecules, such particles do not diffuse. The rate of change of any property of a material particle is given by the substantial derivative. When the property is age, its rate of change is unity. Therefore, letting a_p denote the particle age, which may be set to zero at the inlet to the flow domain

$$\frac{Da_p}{Dt} = \frac{\partial a_p}{\partial t} + \mathbf{v} \cdot \nabla a_p = 1 \tag{19}$$

The material particle has a deterministic age; it does not have a frequency distribution with mean and higher moments. Thus, the age appearing in Eq. 19 is the particle age, not the mean age a. Jongen[13] called a_p the advective age in studying age distribution in unsteady and enclosed flow systems by adding source terms to Eq. 19. Equation 19 differs from Eq. 13 in three other important aspects. First, it can be applied to unsteady flow. Second, it is not restricted to incompressible flows. Third, it lacks a diffusion term. This last difference has major consequences, as in the following discussion.

For steady incompressible flow, Eq. 19 becomes

$$\mathbf{v} \cdot \nabla a_p = \nabla \cdot (\mathbf{v} a_p) = 1 \tag{20}$$

Without a diffusion term, Eq. 20 is a first-order partial differential equation, where the solution is propagated along characteristic curves which are the streamlines of the flow. Only one boundary condition may be applied along any given streamline. It is natural to set the age equal to zero where streamlines emanate from the inlet to the flow. Then, no boundary condition may be applied where these streamlines reach the outlet. The zero normal gradient outlet condition applied to Eq. 13 is in fact contradictory to Eq. 20. The behavior near walls merits discussion. For streamlines emanating from the inlet plane and following close to a wall, in the limit as the wall is approached, the velocity goes to zero and the time required for the fluid particle to reach any downstream position on the wall is infinite. Thus, the age on the wall is infinite. This is no surprise, and is consistent for example with the textbook solution for residence time distribution for laminar flow without diffusion in a tube (see e.g., Middleman[14]). By writing Eq. 20 for a 2-D flow in terms of tangential and normal components near the wall

$$v_t \frac{\partial a_p}{\partial x_t} + v_n \frac{\partial a_p}{\partial x_n} = 1 \tag{21}$$

where x_t and x_n are coordinates in the tangential and normal directions, respectively, it can be seen that in the limit as the wall is approached, both velocity components go to zero so

that either $\partial a_p/\partial x_t$ or $\partial a_p/\partial x_n$ must be infinite. Starting from any interior point in the flow where the age is finite, and following a normal to the wall, infinite age is reached in a finite distance. Therefore, the normal gradient of age must become infinite.

Not all streamlines will intersect the inlet when completely separated flow regions occur. No material particles enter or leave such zones, and age will not propagate into them from the inlet. Finite solutions to Eqs. 19 and 20 do not exist in regions with closed loop streamlines. Starting with a finite age at any point on a closed streamline, the increasing age along the streamline would produce a contradictory age upon completing the loop back to the starting point. Without diffusion, the age must diverge to infinity in such regions. If diffusion were taken into account, such dead zones would have large, but finite age. Without diffusion, the mean age at the exit will be smaller due to the complete bypassing of recirculation zones. Numerical solution of Eq. 20 will introduce numerical diffusion precluding infinite age, but the age inside recirculation zones will still be unrealistically large when grid refinement results in numerical diffusion which is less than molecular or turbulent diffusion.

Equation 20 is based on the same kinematic concept as Lagrangian particle tracking, where $D\mathbf{x}_p/Dt = \mathbf{v}$ is solved along particle paths. In this method, the same challenge of properly defining boundary conditions on solid walls exits. Due to numerical errors of finite resolution of the velocity field near the wall, particles may hit the wall or even leave the flow domain. Some numerical tricks, none of them physically correct, have to be used to retain these particles in the flow domain. The numerical errors introduced by these tricks may affect the statistics of particle age distribution. These challenges of near wall behavior are due to the assumption that particles are purely convected without diffusion. Far from walls, diffusion may be negligible compared to convection. However, near walls diffusion becomes dominant due to the no-slip condition. Therefore, the assumption of negligible diffusion breaks down near solid walls, whether in the Eulerian frame of Eq. 20, or in the Lagrangian frame of particle tracking.

CFD methods based on second-order conservation equations may be applied to Eq. 20 by setting the diffusivity to zero. Numerical diffusion will render the age finite on walls and in recirculation zones. Because they are based on second-order equations, CFD codes require outlet and wall boundary conditions, even though mathematically they are not appropriate to the first-order equation. Fortunately, the outlet boundary condition does not affect the upstream solution for the finite volume method used in this work in its conservative form as long as the flow is convection dominated at the outlet (large Peclet number), and the outlet is chosen such that no backflow occurs.[15]

In a turbulent flow, the age of material particles occupying a fixed point in space will fluctuate with time. Reynolds averaging of Eq. 20 results in a transport equation for the Reynolds averaged particle age, and a turbulent diffusion term results from the covariance of velocity and age fluctuations. For a steady incompressible turbulent flow, the result is

$$\mathbf{v}\cdot\nabla a_p = \nabla\cdot(\mathbf{v}a_p) = \nabla\cdot\left[\frac{\nu_t}{Sc_p}\nabla a_p\right] + 1 \tag{22}$$

This equation for particle age is of the same form as Eq. 13 for the mean age by the tracer method, except that it lacks a molecular diffusion term because material particles are not molecules. It may be useful to include molecular diffusion in Eq. 22 in an *ad hoc* manner, producing a transport equation for the mean molecular age instead of material particle age. In most turbulent flows, molecular diffusion is several orders of magnitude smaller than turbulent diffusion. The addition of the molecular diffusion term will not affect the solution for a_p in the main flow but may become important when the viscous sublayer at the wall is to be resolved. With diffusion included, the same wall and outlet boundary conditions used for Eq. 13 may be applied to Eq. 22, and the age will remain finite. With molecular diffusion terms included, Eq. 22 and its boundary conditions are identical to Eq. 13 and its boundary conditions, and a_p becomes identical to, and is replaced by, the mean molecular age a.

Higher moments of age

Mean age is the first moment of the tracer age distribution function $C(\mathbf{x},t)/I$. Higher moments provide important additional information about the properties of the function. For example, the second moment characterizes the spread of $C(\mathbf{x},t)/I$, and the third moment describes the skewness.

The second moment about the origin is defined as

$$M_2 = \frac{\int_0^\infty t^2 C(\mathbf{x},t)dt}{\int_0^\infty C(\mathbf{x},t)dt} \tag{23}$$

The variance σ^2 is given by the second moment about the mean age

$$\sigma^2 = \frac{\int_0^\infty (t-a)^2 C(\mathbf{x},t)dt}{\int_0^\infty C(\mathbf{x},t)dt} = M_2 - a^2 \tag{24}$$

The coefficient of variation CoV is the square root of the normalized variance. It is a measure of the breadth of the distribution

$$CoV = \sqrt{\frac{M_2 - a^2}{a^2}} \tag{25}$$

Higher moments are similarly defined. The n-th moment about the origin is

$$M_n = \frac{\int_0^\infty t^n C(\mathbf{x},t)dt}{\int_0^\infty C(\mathbf{x},t)dt} \tag{26}$$

All moments are functions of spatial position only.

Transport equations for moments can be derived in the same way as the mean age transport equation, by multiplying tracer concentration equation (Eq. 7) by t^n and time integrating. The equation for the second moment is.

$$\nabla\cdot(\mathbf{v}M_2) = \nabla\cdot(D\nabla M_2) + 2a \tag{27}$$

The equation for the n-th moment is

$$\nabla \cdot (\mathbf{v}M_n) = \nabla \cdot (D\nabla M_n) + nM_{n-1} \tag{28}$$

Following the same steps as in deriving boundary conditions for mean age, the same boundary conditions as Eqs. 14–16 for moments with M_n replacing a are obtained. In deriving the moment equations, it is assumed that $t^n C \to 0$ as $t \to \infty$. As noted for the mean age, this behavior must be obeyed not only for these transport equations to be correct, but also for the moments themselves to exist. Numerical solutions of the transient tracer response C reported later confirmed the validity of this assumption.

In principle, with the solutions of the equations for mean age and higher moments, the distribution function of $C(\boldsymbol{x},t)$ can be fully described. Thus, the full frequency function $\tilde{f}(\mathbf{x},\alpha)$ and the RTD could be determined. Some of the methods for reconstructing a function from moments are discussed by Diemer and Olson,[16] Alopaeus et al.[17] and John et al.[18] For most mixing applications, sufficient process understanding may be gained without full determination of the frequency distribution for age; a few lower moments should be sufficient. For example, CoV is widely used in characterizing mixing conditions in industrial mixing devices.

From Eqs. 12, 24 and 27 the governing equation for σ^2 can be obtained.

$$\nabla \cdot (\mathbf{v}\sigma^2) = \nabla \cdot (D\nabla\sigma^2) + 2D(\nabla a)^2 \tag{29}$$

It is interesting to notice the dissipation-like source term in this equation. The non-negative source term causes the dissipation of an initial pulse. Without diffusion, the initial pulse would remain a pulse as it is convected throughout the flow field.

Relationship between moments of age and residence-time distributions

The mean residence time $\bar{t}$ for steady incompressible flow with closed inlet and outlet is equal to V/Q. Equation 17, derived from the age transport equation, showed that for the same conditions, the mixing-cup mean age $\bar{a}_e$ is also equal to V/Q; thus, the mixing-cup mean exit age and the mean residence time are identical. It is simple to show that this equality follows from the definitions of $\bar{t}$ and $\bar{a}_e$, and that the higher moments of residence time and mixing-cup exit age are also identical. That is, $\overline{t^n} = \overline{M_{n,e}}$.

The mixing cup concentration at the exit is

$$C_{\text{out}}(t) = \frac{\int_{S_e} uC(\mathbf{x},t)dA}{\int_{S_e} C(\mathbf{x},t)dA} = \frac{1}{Q}\int_{S_e} uC(\mathbf{x},t)dA \tag{30}$$

where u is the velocity component normal to the exit surface.

The n-th moment of the residence time is

$$\overline{t^n} = \int_0^\infty t^n f(t)dt = \frac{\int_0^\infty t^n C_{\text{out}}(t)dt}{\int_0^\infty C_{\text{out}}(t)dt} = \frac{\int_0^\infty t^n \int_{S_e} uC(\mathbf{x},t)dAdt}{\int_0^\infty \int_{S_e} uC(\mathbf{x},t)dAdt}$$
$$= \frac{\int_{S_e} u\left[\int_0^\infty t^n C(\mathbf{x},t)dt / \int_0^\infty C(\mathbf{x},t)dt\right]dA}{\int_{S_e} udA} = \frac{\int_{S_e} uM_n dA}{\int_{S_e} udA} = \overline{M_{n,e}} \tag{31}$$

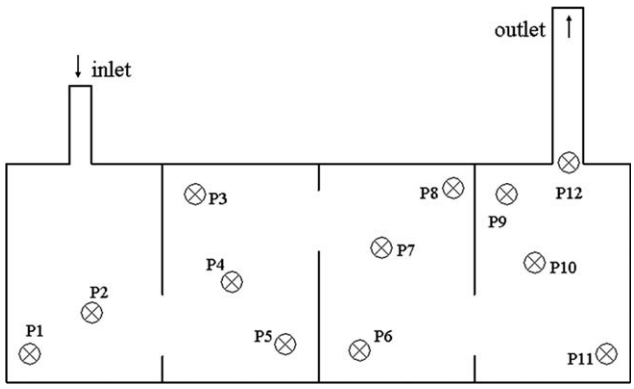

Figure 1. Geometry of the 2-D test reactor.

The marks are the locations of selected points for comparisons of numerical solutions listed in Table 1.

The spatial invariance of $I = \int_0^\infty C(\mathbf{x},t)dt$ has been used in Eq. 31. The mean residence time and mixing cup averaged mean exit age (first moment), and all higher moment pairs of residence time and exit age are identical. All the moments of the RTD f curve (E-curve) can be computed from the moment solutions evaluated at the exit.

CFD model and solution for a 2-D test flow system

A 2-D test problem was constructed to investigate the spatial variation of mean age and higher moments using CFD. The flow domain is of a common reactor style consisting of four equal volume zones separated by baffles, as shown in Figure 1. The choice of a 2-D flow rather than a 3-D flow was made primarily due to the cost of computation. Very little computational effort is needed to obtain the mean age distribution, even for 3-D flows, once the steady-flow field has been obtained. However, in this test problem, mean age and higher moments computed from steady transport Eqs. 12 and 28 are compared with those from the far more computing intensive solutions of the transient tracer transport Eq. 7. In order to track an initial pulse until the entire tracer leaves the system, the unsteady solution needs to be carried out for a time an order of magnitude longer than the mean residence time. The required CPU time even for a 2-D flow is then not trivial. The particular 2-D geometry was chosen to contain features commonly found in more general 3-D flows, such as an inlet jet, separation, dead zones and short-circuiting paths, to show the power of the approach, and to develop insights that should carry over into 3-D problems. For 3-D problems, the solution of the mean age and higher moment transport equations adds extremely small computational burden to that required to generate the velocity field.

The reactor is 2.0 m in length by 0.7 m in height. The inlet dimension is 0.071 m, and outlet is 0.1 m. Air is fed at the inlet at a constant velocity of 20 m/s. The density of the air is 1.225 kg/m^3, and its viscosity is 1.8×10^{-5} kg/m-s. For unit depth, the volume is 1.4679 m^3, and the volumetric flow rate is 1.4280 m^3/s. This results in a mean residence time $V/Q = 1.0279$ s. The Reynolds number in the inlet is about 10^5, and in the interior of the reactor is about 10^4 based on the width of the four zones as the length scale. This puts the flow in the reactor in the turbulent regime. A

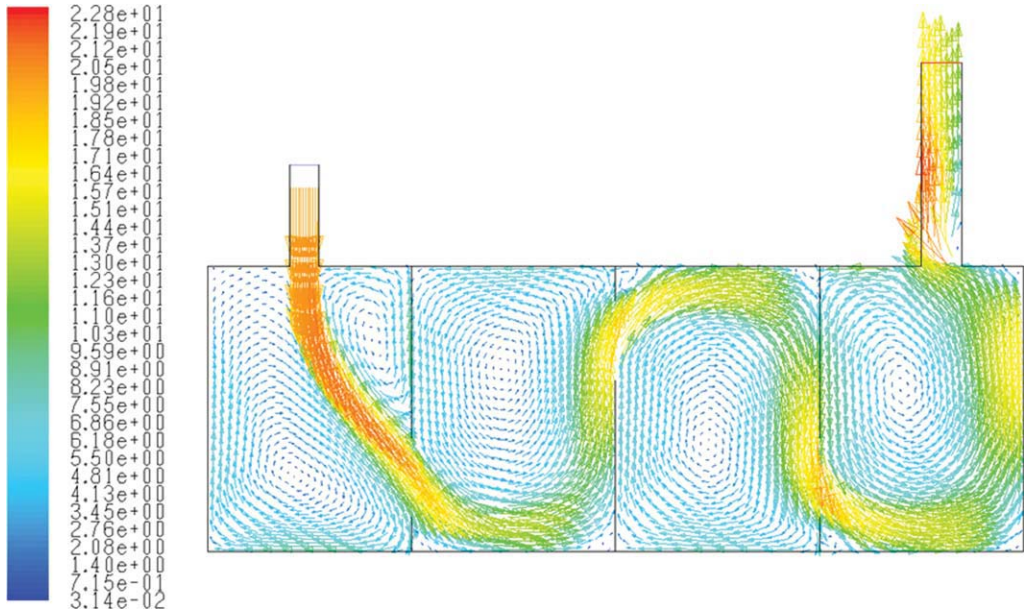

Figure 2. Velocity vector plot of the steady-flow solution in the test reactor.

[Color figure can be viewed in the online issue, which is available at wileyonlinelibrary.com.]

standard k-ε model was used for the turbulence. With such a RANS (Reynolds-averaged Navier-Stokes) model, all small and time-dependent scales in the flow are modeled with large turbulent diffusivity. Thus, the resulting flow solution has no small-scale structures, and it is not necessary to use a fine mesh as typically used for large eddy simulation (LES), or fully resolved direct numerical simulation (DNS) models to resolve any small scales existing in typical turbulent flows. The flow field was solved using the commercial CFD code Fluent™, version 6.3. The total number of cells used in the flow domain was just less than 6,000, all being quad cells.

Velocity field solution

The velocity vector plot is shown in Figure 2. The solution clearly reveals the recirculation regions and the high velocity path generated by the inlet jet. The jet decays as it passes through the reactor due to strong turbulent dissipation. There are two recirculation regions in the first zone of the reactor. The remaining three zones each have only one recirculation region. The high-velocity path stays close to the reactor walls after it passes the first baffle. In many respects these dead zones and short-circuiting paths are typical manifestations of what might be perceived as poor designs for mixing. However, as shall become clear, such interpretations deduced from velocity vector plots may be invalid.

Solutions for mean age and higher moments

Mean age and higher moments were solved from Eqs. 12 and 28 with user-defined scalars in Fluent™. Since each higher moment requires its previous lower moment as a source term, the moments were solved sequentially, starting from the mean age. The turbulent Schmidt number for age S_{ca}, was set to unity. Since the governing equations are linear, the solution process is extremely fast. The CPU time spent on each solution was only about 1 min, compared with many hours for a time-dependent solution of the tracer species conservation equation (Eq. 7).

A contour plot of mean age is presented in Figure 3. As expected, the plot clearly shows the size and location of dead zones. Inside dead zones, mean age is large. The short circuiting path is easily distinguishable with smaller mean age. In practice, knowledge of the spatial mean age distribution, in comparison with characteristic time scales for desired reactions and undesired side reactions, may prove much more useful for assessing reactor performance than the velocity vector plot in Figure 2. The mixing cup averaged mean age at the exit is $\overline{a}_e = 1.0279$ s, identical to four digits beyond the decimal point to the mean residence time calculated from V/Q. At the center of the "dead" zone in zone 4, the maximum mean age is 1.18 s, only 15% greater than $\overline{t}$. Due to high rates of turbulent diffusion between the short-circuiting paths and the dead zones, the variation in age, particularly in the fourth zone, is rather small. The recirculation zones, or "dead zones", are not so dead after all. At the center of the fourth recirculation "dead" zone, the turbulent diffusivity is about 0.1225 m^2/s, about four orders of magnitude greater than the molecular diffusivity. With this strong diffusion, scalars are diffused into and out of the recirculation zones across the streamlines at very high rates. The maximum value of mean age occurs not at the exit but at the center of the last recirculation zone. This possibly counterintuitive behavior is the result of mixing of young and old molecules on their way to the exit. Individual molecules diffusing out of the recirculation zone do not become younger as they flow to the exit; they simply mix with younger ones. When interpreting mean age solutions, it is always important to remember that $a(\mathbf{x})$ is the mean age of molecules of different ages occupying the same point $\mathbf{x}$, not the age of a single molecule.

The ability to show exact sizes and positions of dead zones and short circuiting paths inside the reactor makes the

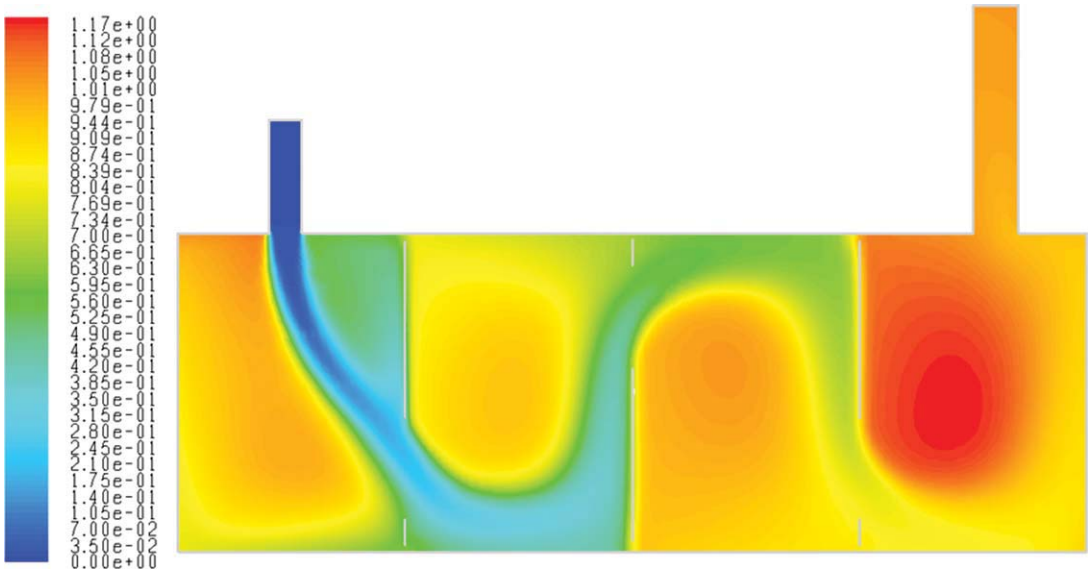

Figure 3. Contour plot of mean age.

mean age method a powerful tool to analyze mixing conditions. By comparison, the (exit) RTD reveals no information about the spatial variation of conditions inside the reactor.

Higher moments up to the fifth were also computed and their spatial distribution patterns were found to be the same as that of mean age but with higher values. The distribution of the normalized variance $(CoV)^2 = \sigma^2/a^2$ was found to be very different. Figure 4 shows the contour plot of normalized variance. Perhaps counterintuitively, the variance is much greater on the short circuiting path than in the dead zones. In fact, it is the greatest in the shear layers of the initial jet. Further insight into this behavior was obtained from the solution of the transient tracer species equation.

Solution of the time-dependent tracer conservation equation

In order to validate the steady transport Eqs. 12 and 28 against the full transient tracer species solution method, based on Eqs. 4 and 7, and to gain more insight on how mean age can be used to analyze the mixing process inside the reactor, numerical solutions by the two methods were compared. For the transient tracer simulation, a constant time step of 0.0002 s was employed. A pulse of pure tracer (mass fraction unity) was supplied at the inlet for a very short period of time, equal to 50 time steps or 0.01 s. The spatial invariant evaluated at the inlet is thus $I/\rho = \int_0^\infty C dt/\rho = 0.01$ s. This value can be used to check

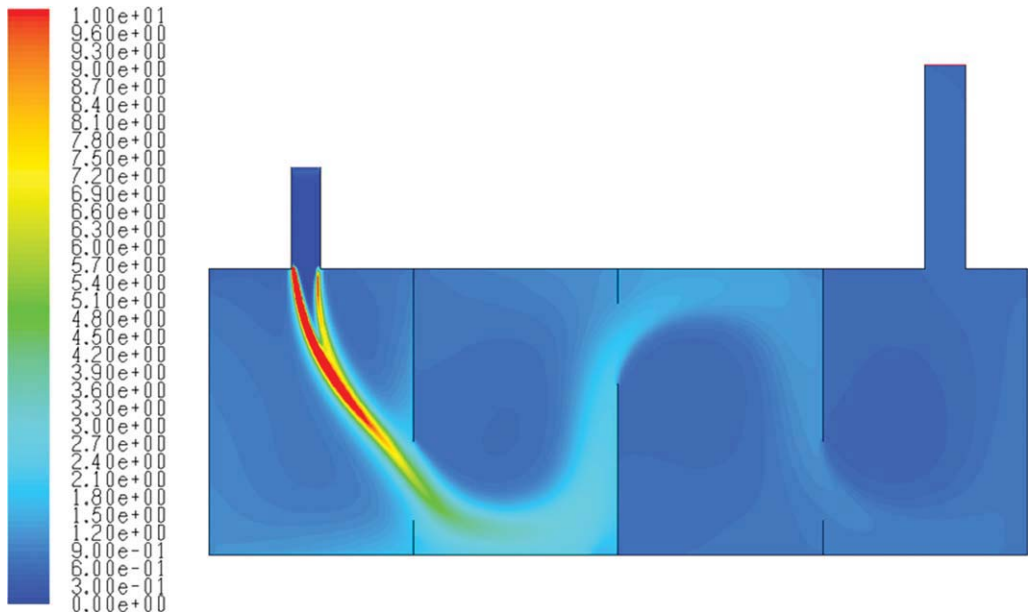

Figure 4. Contour plot of $(CoV)^2$.

Table 1. Comparisons of Transient Tracer Simulations and Moment Transport Equation Results

P(x,y)	a_t, s	a, s	$\overline{t^2}$, s^2	M_2, s^2	$\overline{t^3}$, s^3	M_3, s^3	$(I/\rho) \times 10^2$ s
P1(0.07,0.09)	0.8643	0.8679	1.4758	1.5176	3.6765	3.9702	1.0141
P2(0.27,0.22)	1.0001	1.0110	1.7398	1.8032	4.3373	4.7334	1.0169
P3(0.6,0.6)	0.8582	0.8658	1.2844	1.3153	2.8183	2.9185	1.0013
P4(0.72,0.32)	0.9821	0.9900	1.5188	1.5542	3.3433	3.4185	1.0022
P5(0.89,0.12)	0.3487	0.3558	0.4544	0.4655	1.0371	1.1454	0.9848
P6(1.13,0.1)	0.9649	0.9659	1.5262	1.5489	3.4789	3.6859	0.9974
P7(0.2,0.03)	1.0444	1.0482	1.6905	1.7210	3.8681	4.0585	0.9967
P8(1.43,0.62)	0.6095	0.6160	0.8472	0.8680	1.8888	2.0572	0.9995
P9(1.6,0.6)	1.1076	1.1119	1.8626	1.8984	4.3387	4.5791	0.9984
P10(1.69,0.38)	1.1690	1.1748	2.0062	2.0475	4.7004	4.9368	0.9982
P11(1.92,0.09)	0.8562	0.8649	1.3105	1.3478	2.9764	3.2453	0.9986
P12(1.8,0.7)	0.9823	0.9903	1.5749	1.6139	3.6183	3.8793	0.9990

the accuracy of the numerical solution. The integral I/ρ at any position should have a value close to 0.01 s. Equation 7 was solved using a second-order implicit time integration scheme. For an implicit scheme, the solver is unconditionally stable for any value of the CFL number, which is defined as $u\Delta t/\Delta x$, where u is the velocity magnitude, Δt is the time step, and Δx is the grid spacing. However, small CFL is critical to the accurate time-dependent solution for $C(\mathbf{x},t)$. For the time-step size of 0.0002 s, the mesh CFL number is around 0.3 in the inlet and much smaller in the interior of the reactor. The total physical time of the solution was 12 s, or 60,000 time steps. Using one processor of a Dell Linux workstation (Precision 490 with Xeon chip), the total CPU time was about 8 h to solve the tracer equation after the velocity field was obtained. Time histories of strategically selected locations were recorded for post processing. Twelve points were selected as shown in Figure 1. The points are spread out in all four zones and placed in the short circuiting paths, the dead zones, and the opposite corners from the short circuiting paths. The time history data were then processed with a user-written code outside of Fluent™.

Table 1 lists some statistics at the 12 points. The second column shows the mean age a_t, s computed from the transient tracer simulation. The third column shows the mean age a computed from the steady transport (Eq. 12). The maximum difference is 2% and most agree to within less than 1%. This is a clear indication that the numerical solutions of both methods are accurate. The second moments about the origin from the two methods are listed in the next two columns. Slightly larger differences are noticed, but all are still within 3%. The third moments are listed in the sixth and seventh columns. Again, the agreement is still very good, but the differences increase with increasing moment. At some points, it is more than 10%. The spatial invariant I is listed in the last column. All the values are within 2% of 0.01, confirming its spatial invariance and the accuracy of the solutions.

Figure 5 shows three C-curves at points 3, 4, and 5, all in Zone 2. Each of the three points represents a different region of flow. Point 5 is on the short circuiting path, Point 4 is near the center of the dead zone, and Point 3 is in the recirculation zone but far away from dead center and the short circuiting path. The mean age is also shown. As can be seen, the mean age occurs well after the peak. The most unexpected one is at Point 5, shown in Figure 5c where the mean age is far away from peak and on the long tail. The peak is at about $t = 0.075$ s, which is the time the main pulse arrives. The mean age is $a = 0.3558$ s, which is 4.7 times the peak age. The mean ages at Points 3 and 4 are also quite far from their peaks as shown in Figure 5a and 5b. The ratios of mean age to peak age are 4.2 and 3.2, respectively. The large ratio of mean age to peak age is the result of the long tail. One might expect a long tail when diffusion dominates the transport of the scalar but not when convection is dominant, such as at Point 5. The result at Point 5 shows that even when convection is dominant, diffusion from nearby recirculation zones can also contribute to the development of a long tail.

To further characterize the scalar concentration curves, CoV and skewness $S_k = k^{1/3}$ were computed. At Point 5, CoV = 1.674, at Point 4, CoV = 0.6981, and at Point 3, CoV = 0.8746. Thus, C is more spread out in the convection dominated region than in the diffusion dominated region. It is the long tail that gives this unexpected behavior. Skewness about mean age is defined as the one third-power of

$$k(\mathbf{x}) = \frac{\int_0^\infty (t-a)^3 C(\mathbf{x},t)dt}{a^3} \tag{32}$$

Skewness is a measure of asymmetry of the distribution. Positive skewness indicates that the long-age tail is larger than the small-age tail. Large positive skewness values were obtained at all the test points, due to the long tails. At Point 5, $S_k = 2.56$, at Point 4, $S_k = 0.98$, and at Point 3, $S_k = 1.12$, indicating the peak is far left of the mean value. Danckwerts[8] was concerned with the uncertainty in the determination of mean residence time caused by the difficulty in measuring long tails, and suggested using the median residence time $t_{1/2}$ defined by

$$I = 2\int_0^{t_{1/2}} C_{\text{out}}(t)dt \tag{33}$$

At any local point in the flow field, the median age $a_{1/2}$ may be similarly defined by

$$I = 2\int_0^{a_{1/2}} C(\mathbf{x},t)dt \tag{34}$$

Half of the total molecules passing through $\mathbf{x}$ have age less than the median. For some purposes, the median age

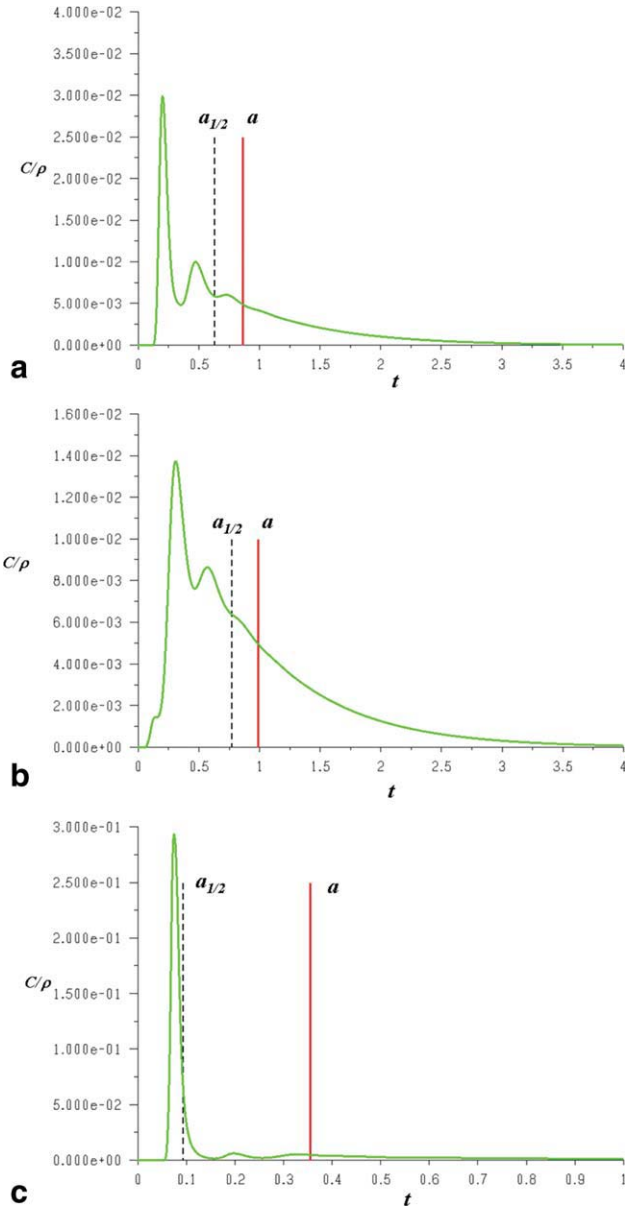

Figure 5. (a) Time history of tracer concentration at point 3. a = 0.8658 s, and $a_{1/2}$ = 0.6323 s. (b) Time history of tracer concentration at point 4. a = 0.9900 s, and $a_{1/2}$ = 0.7645 s. (c) Time history of tracer concentration at point 5. a = 0.3558 s, $a_{1/2}$ = 0.0863 s.

[Color figure can be viewed in the online issue, which is available at wileyonlinelibrary.com.]

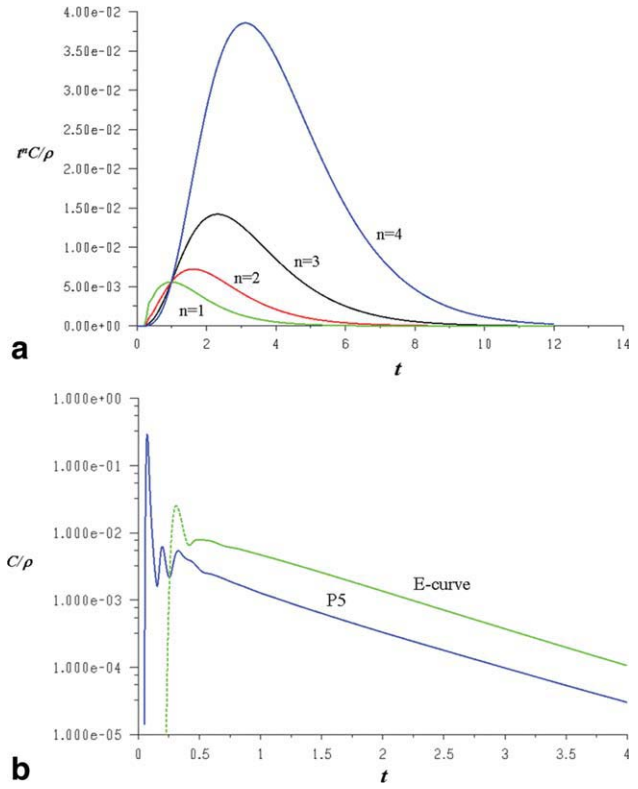

Figure 6. (a) t^nC as functions of time at point 4. n = 1, 2, 3, 4. All t^nC decay exponentially after reaching peak value. (b) Semilog plots of concentration at point 5 and E-curve showing exponential tails.

[Color figure can be viewed in the online issue, which is available at wileyonlinelibrary.com.]

may be preferable to the mean age as a representation of the average age. The median age is also plotted in Figure 5. For all three curves, the median age comes closer to the peak age than does the mean age.

In deriving Eqs. 12 and 28, it has been assumed that $t^nC \rightarrow 0$ as $t \rightarrow \infty$, with an expectation that C decreases exponentially at long time. Figure 6a shows the results of numerical tests of this assumption. Four curves of t^nC with n up to 4 calculated at point 4 are shown. The curves confirm the assumed behavior. Figure 6b shows the C-curve from Figure 5c, but in semilog scale. Also shown in this figure is the E-curve at the exit. It can be seen clearly that these curves have exponential tails.

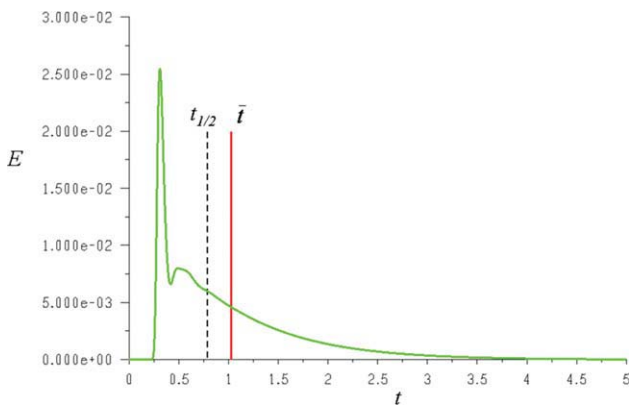

Figure 7. E-curve at the exit, computed according to Eqs. 1 and 30.

$t_{1/2}$ = 0.7865 s. Mean residence time $\bar{t}_{1/2}$ = 1.0266 s. [Color figure can be viewed in the online issue, which is available at wileyonlinelibrary.com.]

The E-curve or frequency distribution f computed by Eq. 1 from the tracer transient species balance is shown in Figure 7. Also shown in the figure is the mean residence time $\bar{t} = 1.0266$, computed from Eq. 3. This is very close to $V/Q = 1.0279$ s.

The mean residence time from Eq. 3 should be close to V/Q as long as the solution has been carried out for long enough time for all the material in the pulse to exit. The numerical results show that at $t = 2\bar{t}$, the computed mean residence time is within 10% of $\bar{t}$; at $t = 4\bar{t}$, it is within 4%; at $t = 6\bar{t}$, it is within 1%. For higher moments, the waiting time needs to be longer, because the error caused by cutting the E-curve tail too early is greater due to the magnifying effect of t^n and the shift of the peak of the $t^n f$ curve, as shown in Figure 6a. For example, the error from $\overline{M_{3,e}}$ for the third moment $\overline{t^3}$ at $t = 2\bar{t}$ is 71%; at $t = 4\bar{t}$ it is 25%; and at $t = 6\bar{t}$ it is 5.6%. Moments up to the fifth were computed from the E-curve and compared with mass averaged exit values computed from Eq. 28. Excellent agreement was obtained: $\overline{t^2} = 1.6925$ s^2, $\overline{M_{2,e}} = 1.6901$ s^2, $\overline{t^3} = 4.0846$ s^3, $\overline{M_{3,e}} = 4.0666$ s^3, $\overline{t^4} = 13.2324$ s^4, $\overline{M_{4,e}} = 13.1321$ s^4, and $\overline{t^5} = 54.2306$ s^5, $\overline{M_{5,e}} = 53.7661$ s^5.

It may seem natural to assume a direct relationship between the spatial distribution of mean age $a(\mathbf{x})$ at the exit and the residence time distribution $E(t)$ or $f(t)$. That is, one might form a mass-weighted distribution function from the spatial variation of the mean age across the exit plane, such as the previously cited example for the residence-time distribution computed for the parabolic laminar velocity profile in a tube. The distribution so obtained is equal to the residence time distribution only when there is no diffusion. Since the local mean age is an averaged quantity, its mass-flow weighted spatial distribution at the exit may be much narrower than the E-curve. In the current numerical example, the range of mean age across the exit plane is very narrow, from 1.0268 to 1.0321 s. By comparison, the computed residence-time distribution as shown in Figure 7 is much broader, ranging from about 0.25 s to beyond 5 s.

Conclusions

A complete set of conservation (transport) equations and boundary conditions for spatial mean age and higher moments has been derived for steady laminar flows and steady Reynolds averaged turbulent flows. These equations can be solved sequentially from a known velocity field. Compared with the solution of the time-dependent conservation equation for tracer species transport, this set of equations can be solved at only a small fraction of the computing effort. For the 2-D test problem, it took 8 h to obtain the solution for the transient tracer concentration, but only about 1 min of computation time for each moment from the steady transport equations.

A significant advantage of the spatial mean age is that it clearly shows the dead zones and short circuiting paths inside a vessel. The sizes and locations of such zones can easily be obtained by post processing of the solution. By contrast, in the traditional use of residence time distribution, where probability function information is obtained from data only at the vessel exit, the existence of such zones can only be inferred or guessed from the shape of the RTD. The RTD contains no information about the spatial locations of such flow features. These differences make it important to dispel confusion resulting from variations in terminology and description of age and residence time in the literature. Often these terms are used interchangeably. In this article, the convention explained and followed is that residence time refers to the exit plane, and is based on the transient tracer concentration mixing-cup averaged across the exit plane, while age is a spatially varying distribution function which exists at any point within the vessel.

It has been shown that the mass-flow weighted average of the mean age at the exit is equal to the mean residence time. The same is true for all the higher moments. All moments of the residence time distribution can be computed by solving the steady moment transport equations, as a computationally inexpensive alternative to the computationally intensive solution of the transient tracer species conservation equation. The latter becomes especially expensive for the higher moments, where it was found that longer real times must be simulated to obtain accurate solutions.

The RTD is a probability or frequency distribution providing no spatial resolution. The solution of the transport equation for mean age and higher moments provides only the spatial dependence of moments of the frequency distribution, and not the age frequency distribution itself. To obtain the spatially dependent frequency functions, the transient tracer concentration equations must be solved. When this must be done, it is useful to compute moments from the transient tracer response, and compare them to moments computed from the steady transport equations. This provides a way to check that sufficiently small time steps, and sufficiently long real times, have been used in the transient solution.

A 2-D test problem revealed further insights regarding the mean age and higher moment distributions in a steady Reynolds-averaged turbulent flow.

- Short-circuiting paths and relatively dead zones indicated by velocity vector results were examined for mean age and higher moments. The mean age of fluid in the apparently dead zones was mostly within tens of percentage points of the mean age in the adjacent short-circuiting advection dominated zones, indicative of substantial turbulent exchange between zones. Thus, the categorization of low-velocity recirculation zones as "dead" based on examination of the velocity field alone would be a mischaracterization.
- As indicated by CoV computed from the second moment, the frequency distribution of age is broad both in the diffusion dominated recirculation zones and in the advection dominated short-circuiting paths. Diffusion between the zones broadened the distribution in the short-circuiting paths. The CoV in the short-circuiting zones was larger than in the recirculation zones, due to this exchange, which produced very long tails in the short-circuiting zone frequency distributions.
- The distributions were significantly skewed in both zone types, with the mean age located on the long tail. The mean age was much larger than the median age.
- The maximum value of mean age did not occur on the exit plane, but rather in one of the recirculation zones.
- The assumption in the derivation of moment equation that $t^n C(\mathbf{x}, t) \to 0$ as $t \to \infty$, which is a necessary condition for the existence of n-th moment, was numerically confirmed. The numerical results clearly show the exponential decay of C. The spatial invariance of $I = \int_0^\infty C dt$ was also confirmed numerically.

Literature Cited

1. Nauman EB, Residence time distributions. In: Paul EL, Atiemo-Obeng VA, Kresta SM. *Handbook of Industrial Mixing*. New York: John Wiley & Sons, Inc.; 2004:1–17.
2. Nauman EB, Buffham BA. *Mixing in Continuous Flow Systems*. New York: John Wiley & Sons, Inc.; 1983.
3. Levenspiel O. *Chemical Reaction Engineering*. 3rd ed. New York: John Wiley & Sons, Inc.; 1999.
4. Danckwerts PV. Continuous flow systems. Distribution of residence times. *Chem Eng Sci*. 1953;2:1–13.
5. Gilliland ER, Mason EA. Gas mixing in beds of fluidized solids. *Ind Eng Chem*. 1952;44:218–224.
6. Danckwerts PV. The effect of incomplete mixing on homogeneous reactions. *Chem Eng Sci*. 1958;8:93–102.
7. Zwietering TN. The degree of mixing in continuous flow systems. *Chem Eng Sci*. 1959;11:1–15.
8. Danckwerts PV. Local residence-times in continuous-flow systems. *Chem Eng Sci*. 1958;9;78–79.
9. Sandberg M. What is ventilation efficiency? *Build Environ*. 1981;16:123–135.
10. Spalding DB. A note on mean residence-times in steady flows of arbitrary complexity. *Chem Eng Sci*. 1958;9:74–77.
11. Baleo JN, Le Cloirec P. Validating a prediction method of mean residence time spatial distributions. *AIChE J*. 2000;46: 675–683.
12. Froment GF, Bischoff KB. *Chemical reactor analysis and design*. New York: John Wiley & Sons, Inc.; 1979.
13. Jongen T. Extension of the age-of-fluid method to unsteady and closed flow systems. *AIChE J*. 2004;50:2020–2037.
14. Middleman S. *Fundamentals of Polymer Processing*. New York: McGraw-Hill, Inc.; 1977.
15. Patankar SV. *Numerical Heat Transfer and Fluid Flow*. Washington, DC: Hemisphere Publishing Corp.; 1980.
16. Diemer RB, Olson JH. A moment methodology for coagulation and breakage problems: Part 2—Moment models and distribution reconstruction. *Chem Eng Sci*. 2002;57:2211–2228.
17. Alopaeus V, Laakkonen M, Aittamaa, J. Solution of population balances by high order moment-conserving method of classes: reconstruction of a non-negative density distribution. *Chem Eng Sci*. 2008;63:2741–2751.
18. John V, Angelov I, Oncul AA, Thevenin D. Techniques for the reconstruction of a distribution from a finite number of its moments. *Chem Eng Sci*. 2007;62:2890–2904.

Manuscript received Apr. 15, 2009, and final revision received Nov. 5, 2009.